Swelling-induced upregulation of miR-141-3p inhibits hepatocyte proliferation

Authors
Nils Bardeck, Martha Paluschinski, Mirco Castoldi, Claus Kordes, Boris Görg, Jan Stindt, Tom Luedde, Stephan vom Dahl, Dieter Häussinger, David Schöler

Correspondence
david.schoeler@hhu.de (D. Schöler).

Graphical abstract
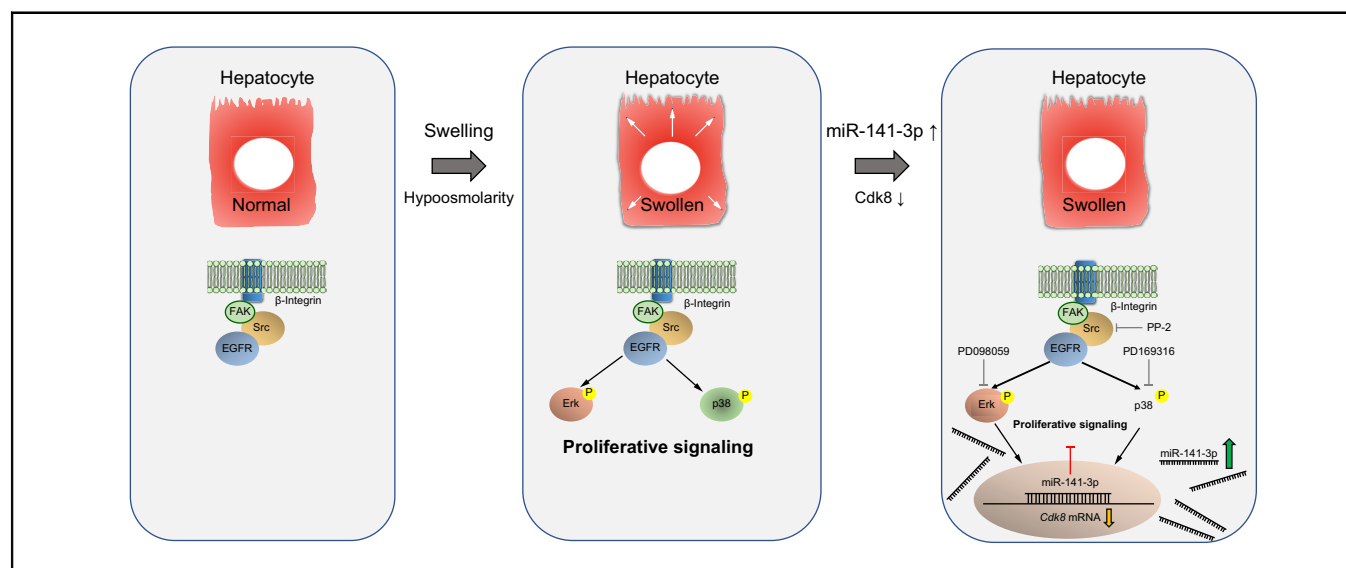
Highlights

- Gene expression changes in hypoosmotic perfused rat liver.

- Hypoosmolarity upregulates miR-141-3p in rat perfused liver and primary hepatocytes.

- Src-/Erk-/p38-MAPK-inhibition prevents miR-141-3p upregulation by hypoosmolarity.

- PHx and hepatocyte stretch transiently upregulate miR-141-3p, which downregulates *Cdk8* mRNA.

- Overexpression of miR-141-3p inhibits Huh7 cell proliferation.

Lay summary
In this study, we identified microRNA 141-3p as an osmosensitive miRNA, which inhibits proliferation during liver cell swelling. Upregulation of microRNA 141-3p, controlled by Src-, Erk-, and p38-MAPK signalling, results in decreased mRNA levels of various genes involved in metabolic processes, macromolecular biosynthesis, and cell cycle progression.

Swelling-induced upregulation of miR-141-3p inhibits hepatocyte proliferation

Nils Bardeck,[1] Martha Paluschinski,[1] Mirco Castoldi,[1] Claus Kordes,[1] Boris Görg,[1] Jan Stindt,[1] Tom Luedde,[1] Stephan vom Dahl,[1] Dieter Häussinger,[1] David Schöler[1,*]

[1]Department of Gastroenterology, Hepatology, and Infectious Diseases, Heinrich Heine University Hospital, Düsseldorf, Germany

Background & Aims: MicroRNAs (miRNAs) act as a regulatory mechanism on a post-transcriptional level by repressing gene transcription/translation and play a central role in the cellular stress response. Osmotic changes occur in a variety of diseases including liver cirrhosis and hepatic encephalopathy. Changes in cell hydration and alterations of the cellular volume are major regulators of cell function and gene expression. In this study, the modulation of hepatic gene expression in response to hypoosmolarity was studied.

Methods: mRNA analyses of normo- and hypoosmotic perfused rat livers by gene expression arrays were used to identify miRNA and their potential target genes associated with cell swelling preceding cell proliferation. Selected miR-141-3p was also investigated in isolated hepatocytes treated with miRNA mimic, cell stretching, and after partial hepatectomy. Inhibitor perfusion studies were performed to unravel signalling pathways responsible for miRNA upregulation.

Results: Using genome-wide transcriptomic analysis, it was shown that hypoosmotic exposure led to differential gene expression in perfused rat liver. Moreover, miR-141-3p was upregulated by hypoosmolarity in perfused rat liver and in primary hepatocytes. In concert with this, miR-141-3p upregulation was prevented after Src-, Erk-, and p38-MAPK inhibition. Furthermore, luciferase reporter assays demonstrated that miR-141-3p targets cyclin dependent kinase 8 (*Cdk8*) mRNA. Partial hepatectomy transiently upregulated miR-141-3p levels just after the initiation of hepatocyte proliferation, whereas *Cdk8* mRNA was downregulated. The mechanical stretching of rat hepatocytes resulted in miR-141-3p upregulation, whereas *Cdk8* mRNA tended to decrease. Notably, the overexpression of miR-141-3p inhibited the proliferation of Huh7 cells.

Conclusions: Src-mediated upregulation of miR-141-3p was found in hepatocytes in response to hypoosmotic swelling and mechanical stretching. Because of its antiproliferative function, miR-141-3p may counter-regulate the proliferative effects triggered by these stimuli.

Lay summary: In this study, we identified microRNA 141-3p as an osmosensitive miRNA, which inhibits proliferation during liver cell swelling. Upregulation of microRNA 141-3p, controlled by Src-, Erk-, and p38-MAPK signalling, results in decreased mRNA levels of various genes involved in metabolic processes, macromolecular biosynthesis, and cell cycle progression.

Introduction

Important physiological functions such as cell proliferation initiation are controlled by alterations in cellular volume, which in turn can be modulated by bile acids, hormones, amino acid intake, or oxidative stress (see reviews[1–5]). Several osmosensing and osmosignalling pathways have been identified, which couple cell volume to cell metabolism, transport, gene expression, proliferation, and apoptosis.[5] For example, cell swelling and shrinkage result in the activation of anabolic or catabolic signalling pathways, respectively.[1,2] We have previously shown that hyperosmotic stress leads to the upregulation of members of the proapoptotic miR-15/107 family and to the downregulation of anti-apoptotic genes, including *Bcl2,* in perfused rat liver.[6] MicroRNAs (miRNAs) modulate diverse cellular processes, such as systemic iron homeostasis,[7] cell proliferation,[8] apoptosis,[9] reactive oxygen species formation[6] and cellular responses to environmental stressors.[10] The dysregulation of miRNA expression has been linked to the biogenesis of several human diseases, including cancer,[11] diabetes,[12] and cholangiopathies.[13] It has been shown that miRNAs participate in the regulation of osmotic stress in zebrafish[14] and control the expression of aquaporin-1 via osmotically sensitive miRNAs (*e.g.* miR-666 and miR-708) in mice.[15] Previously, it was shown that hepatocyte swelling, which can be induced by hypoosmolarity or insulin, triggers hepatocyte proliferation.[16] Hypoosmolarity or insulin-induced hepatocyte swelling initiates an integrin- and c-Src kinase-dependent epidermal growth factor receptor (EGFR) activation.[17] The potential involvement of miRNAs in hepatocyte swelling-associated osmosignalling is largely unknown. Because miRNAs have been reported to often play important roles in metabolic homeostasis

through the regulation of multiple genes, they have attracted interest as diagnostic and prognostic biomarkers. Therefore, the aim of this study was to identify the role of miRNAs and their target genes under hypoosmotic conditions.

Materials and methods

Rat liver perfusion

Rat liver perfusions were conducted as previously described.[18] Perfusion with hypoosmotic medium (225 mOsm/L) was performed by lowering the NaCl concentration to 75 mM in the Krebs–Henseleit buffer. The osmolarity was measured using an Osmomat 3000 (Gonotec, Berlin, Germany). For inhibitor studies, following the preperfusion with normoosmotic medium (305 mOsm/L), Krebs–Henseleit buffer was supplemented with 500 nM PD098059 (Calbiochem, Darmstadt, Germany), 250 nM PP-2 (Calbiochem), 250 nM PD169316 (Santa Cruz Biotechnology, Heidelberg, Germany), or 500 nM colchicine (Thermo Fisher Scientific, Darmstadt, Germany), followed by administration of hypoosmotic medium (225 mOsm/L). Tissue viability was routinely tested by measuring the release of lactate dehydrogenase and portal pressure during perfusion. Over a course of 0–180 min, tissue was dissected and flash frozen.

All experimental protocols were carried out in accordance with the guidelines of the Institutional Animal Care and Use Committee of the University Hospital Düsseldorf, Düsseldorf, Germany. Rat liver perfusion techniques were approved by local officials (LANUV, Landesamt für Natur, Umwelt und Verbraucherschutz, Recklinghausen, Nordrhein-Westfalen, Germany; project number 84-02.04.2015.A287), and all animals received care according to the German animal welfare act.

Affymetrix microarray hybridisation, data analysis, and gene ontology term enrichment

To identify the effect of hypoosmotic perfusion on the liver transcriptome, hepatic RNAs isolated from perfused rat livers at 0, 120, and 180 min (4 independent experiments) were hybridised to Affymetrix GeneChip rat gene 1.0 ST arrays. cDNA synthesis and labelling were performed according to the Affymetrix protocol. Microarray data analyses were performed using the Transcriptome Analysis Console 4.0.2.15 (Thermo Fisher Scientific). The filter criteria were changes of at least 1.5-fold on the linear scale and *p*-value <0.05. Gene ontology (GO) term enrichment of biological processes was performed using GOrilla.[19]

Partial hepatectomy

The surgical removal of an estimated 70% of liver mass (median lobe and left lateral lobe) was conducted on male Wistar rats (8–10 weeks old, approximately 250 g body weight) as described.[20] Liver samples were collected during tissue regeneration from 3–6 different animals for the indicated time points and analysed by qPCR and miQPCR. The animal experiments were approved by the LANUV (project number 9.93.2.10.34.07.163).

Preparation and cultivation of rat primary hepatocytes

Hepatocytes were isolated from the livers of male Wistar rats (160–180 g) by a modified collagenase perfusion technique, described previously.[21] Cultured rat primary hepatocytes were treated with normoosmotic or hypoosmotic medium in the presence or absence of 10 μM PP-2 (Calbiochem, Darmstadt,

Germany), 10 μM PD098059 (Calbiochem), or 10 μM PD169316 (Santa Cruz Biotechnology) for up to 24 h. Afterwards, cells were washed with PBS and lysed with QIAzol lysis reagent (Qiagen, Hilden, Germany). The total RNA was extracted via chloroform/ phenol extraction.

Mechanical stimulation of isolated rat primary hepatocytes

Freshly isolated primary rat hepatocytes at Day 2 of culture were exposed to mechanical stimulation in stretch chambers (STREX, San Diego, CA, USA). Stretch chambers were elongated by ∼30% or unstretched (control) over a time of 3 h, respectively. A total of 250,000 hepatocytes were seeded on stretch chambers. Cell stretching was performed unidirectionally, monitored microscopically, and verified by measuring the increased diameter of cell nuclei utilising the software tool cellSens Dimensions (Olympus, Tokyo, Japan). Images were taken using an Olympus IX 50 microscope equipped with a DP71 camera (Olympus). RNA was extracted as described above.

Quantitative real-time PCR (qPCR) analysis

For the mRNA analysis, first-strand cDNA was synthesised from RNA using the RevertAid H Minus First Strand cDNA Synthesis Kit (Thermo Fisher Scientific). qPCR analysis was conducted using Maxima SYBR Green (Thermo Fisher Scientific) and qTOWER[3] (Analytik Jena AG, Jena, Germany) qPCR cycler. The quantification of miRNA was performed by miQPCR.[22] The expression of mRNAs and miRNAs were analysed using qBASE software.[23] The primers used in the miQPCR and qPCR analysis are listed in the Supplementary CTAT methods table.

Transfection of rat primary hepatocytes with miR-143-3p mimic

Freshly isolated rat primary hepatocytes were seeded in sterile 12-well plates as described above. After 24 h, cells were transfected with 25 pmol miR-141-3p mimic (Thermo Fisher Scientific), using Lipofectamine RNAiMAX (Thermo Fisher Scientific) according to the manufacturer's instructions. Control cells were mock-transfected with transfection reagent in the absence of a mimic.

Target prediction analysis

Target prediction analysis was carried out and target genes were analysed according to their potential binding sites for miRNAs in their 3′-UTR. Putative miRNA targets were identified using the miRbase database,[24] the gene database EnsEMBL,[25] MicroCosm Targets (Version 5),[26] and CLC Genomics Workbench (https:// digitalinsights.qiagen.com).

Dual luciferase reporter assay

The full-length sequence of cyclin dependent kinase 8 (*Cdk8*) mRNA 3′-UTR was cloned into the multiple cloning site of a modified *Firefly* luciferase plasmid derived from the pGL3-Promoter vector (Promega, Fitchburg, WI, USA), as previously described.[10] The amplification and insertion of selected 3′-UTRs were carried out with the In-Fusion HD Cloning Kit (Takara Bio, Saint-Germain-en-Laye, France) according to the manufacturer's instructions. In this study, 2 plasmids were generated for *Cdk8* mRNA as a putative target: 1 plasmid with the 3′-UTR sequence in its original orientation (+), and the second with the 3′-UTR sequence in its antisense orientation (-), which functioned as a negative control. Furthermore, the perfect miR-141-3p binding site was likewise cloned into pGL3-derived plasmids to generate

A

120 min hypoosmotic perfusion (225 mOsm/L)

B

180 min hypoosmotic perfusion (225 mOsm/L)

Unchanged
Upregulated
Downregulated

20,850 (~97.4%)

205 (~0.4%)   351 (~1.6%)

20,263 (~94.6%)

609 (~2.8%)   534 (~2.5%)

C

Sample log folds-120

13

7.25

1.5

HYPO_B_120.r... HYPO_A_120.r... HYPO_C_120.r... HYPO_D_120.r... NORM_D_120.r... NORM_B_120.r... NORM_A_120.r... NORM_C_120.r...

D

Sample log folds-180

4

2

0

NORM_B_180.r... NORM_D_180.r... NORM_A_180.r... NORM_C_180.r... HYPO_A_180.r... HYPO_B_180.r... HYPO_D_180.r... HYPO_C_180.r...

Fig. 1. Effect of hypoosmotic exposure on liver transcriptome in perfused rat liver. Rat livers were perfused with normo- (305 mOsm/L) or hypoosmotic (225 mOsm/L) buffer for 120 or 180 min. Following liver dissection, the mRNAs were analysed on Affymetrix GeneChip 1.0 ST. The pie charts illustrate the number of genes significantly altered in hypoosmotic *vs.* normoosmotic liver perfusions after 120 min (A) or 180 min (B). Heat maps of genes with altered expression levels under hypoosmolarity (225 mOsm/L) show a hierarchical clustering representing the differential expression of significantly regulated genes in perfused rat liver when compared with normoosmotic perfused rat liver at time points 120 (C) and 180 min (D). (n = 4; threshold of 1.5-fold; significance level p = 0.05; 1-way ANOVA.)

a positive [pMir(+) 141-3p] and a negative [pMir(-) 141-3p] control plasmid. HEK293 cells were seeded in sterile 12-well plates (80,000 cells per well). Transfection was performed with Lipofectamine 3000 (Thermo Fisher Scientific) according to the manufacturer's instructions. Cells were harvested for the Dual-Luciferase Reporter Assay[27] 24 h post-transfection and measured in a GloMax Multi Plus Multiplate Reader (Promega, Waldorf, Germany). The relative activity of the *Firefly* luciferase from cells transfected with miR-141-3p mimic was compared with mock transfected cells (control); the latter was set to 100%.

Primer design

miRNA sequences were acquired from http://www.mirbase.org (Version 22.1). Melting temperatures for miRNA primers were calculated using the Oligo Explorer 1.1.2 tool (http://www.genelink.com/tools/gl-oe.asp). mRNA primers were designed and assessed by the Roche Universal ProbeLibrary Assay Design Center (https://lifescience.roche.com/en_de/brands/universal-probe-library.html#assay-design-center) with respect to their secondary structure, possible self-dimerisation, and primer duplexes. TargetScanHuman 7.2 at http://www.targetscan.org/

vert_72/ and miRWalk 3.0 at http://mirwalk.umm.uni-heidelberg.de/ were used for target prediction and genomic DNA, and the 3′-UTR sequences were obtained from the Ensembl Gene database 93 at http://www.ensembl.org/biomart/martview/.

Huh7 cell viability and proliferation

To measure Huh7 cell viability and proliferation, 1.4×10^4 Huh7 cells (passages 30, 32–34) were seeded per 6-well cavity (Greiner Bio-One, Solingen, Germany) and cultured for 24 h in DMEM/F12 (Thermo Fisher Scientific) containing 10% FBS (PAN Biotech, #P30-3031). Cells were washed twice in DMEM/F12 and transfected without (mock) or with miR-141-3p mimic for 5 h in DMEM/F12 without FBS as described above. At the end of the incubation period, cells were washed twice with DMEM/F12 and cultured for another 48 h in DMEM/F12 containing 10% FBS. As control, Huh7 cells were cultured for 48 h in DMEM/F12, with or without 10% FBS.

Huh7 cell viability was measured by incubating Huh7 cells with propidium iodide (Sigma-Aldrich, Deisenhofen, Germany, #P4864, 1:250) and Hoechst 34580 (Thermo Fisher Scientific,
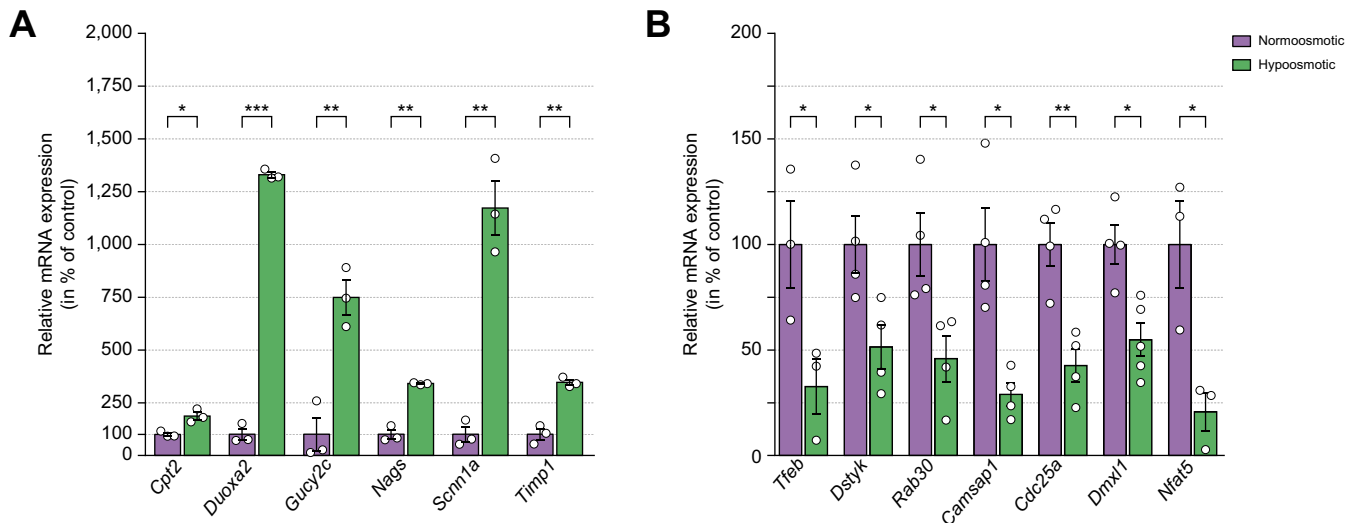
Fig. 2. qPCR validation of selected mRNAs in rat liver perfused with normo- or hypoosmotic medium. Validation of selected upregulated (A) and down-regulated (B) mRNAs in rat liver perfused with normo- (305 mOsm/L) or hypoosmotic medium (225 mOsm/L). Rat livers were perfused for 180 min, livers were dissected, and the mRNA was analysed by qPCR (n = 4–5). qPCR data were median-normalised. Statistical analysis was carried out using the Student t test. Data are shown as mean ± SEM with *$p < 0.05$, **$p < 0.01$, and ***$p < 0.001$. *Camsap1*, calmodulin-regulated spectrin-associated protein 1; *Cdc25a*, cell division cycle 25A; *Cpt2*, carnitine palmitoyl transferase 2; *Dmxl1*, Dmx Like 1; *Dstyk*, dual serine/threonine and tyrosine protein kinase; *Duoxa2*, dual oxidase maturation factor 2; *Gucy2c*, guanylate cyclase 2C; *Nags*, N-acetyl glutamate synthase; *Nfat5*, nuclear factor of activated t cells 5; *Rab30*, member RAS Oncogene Family; *Scnn1a*, sodium channel epithelial 1 subunit alpha; *Tfeb*, transcription factor EB; *Timp1*, tissue inhibitor of metalloproteinase 1.

#H21486, 1:5,000) for 15 min at 37°C and 5% CO_2. Cells were washed twice with DMEM/F12 and mounted on an Axio Observer Z1 (Carl Zeiss AG, Oberkochen, Germany). Images were acquired using an EC Plan-Neofluar 10×/0.30 Ph 1 objective, an AxioCamMR3_2, and AxioVision Software (Carl Zeiss AG). Propidium iodide fluorescence intensities were measured using the FIDJI distribution of ImageJ.[28] Fluorescence intensities found in miRNA-mimic-transfected cells or cells cultured without FBS are given relative to mock-transfected or Huh7 cells cultured in DMEM/F12 with FBS, respectively. Proliferation was measured by fluorimetric quantification of the DNA content.[29] For this, culture medium was removed, and cells were fixed with freshly prepared 4% paraformaldehyde (Thermo Fisher Scientific, #28906) for 5 min at room temperature (RT). DNA was stained for 15 min at RT with Hoechst 34580 (Thermo Fisher Scientific, #H21486) diluted 1:5,000 in PBS (PAN Biotech, Aidenbach, Germany, #P04-36500). Excess dye was removed by washing the cells 3 times with PBS. Hoechst 34580 fluorescence was measured using a Fluoroscan Ascent FL fluorimeter (Thermo Fisher Scientific) with an excitation and emission wavelength maxima of 380 and 460 nm, respectively. Fluorescence intensities were corrected for background fluorescence (unstained cells) and are given relative to the respective control (mock or DMEM/F12 + 10% FBS).

Flow cytometric analysis of hypoosmolarity-induced swelling of primary rat hepatocytes
Primary rat hepatocytes were prepared by collagenase perfusion as described above. Cell density was established by Neubauer chamber counting, and 500,000 cells were resuspended in 1 ml medium of the indicated osmolarity and incubated for 5 min at 37°C. Cell suspensions were put on ice and 50,000 cells were immediately analysed using a FACSCanto II (Becton Dickinson, NJ, USA) and FACSDiva software V.6.12 (Becton Dickinson, NJ, USA) to

record forward and side scatter. Because the area of the forward scatter (FSC-A) pulse signal generated by a cell is proportional to its size,[30] this technique was used to detect hypoosmotic swelling.

Statistical analysis
Values from different animals or experiments are presented as means and their variations are indicated by the standard error of the mean (±SEM). Comparisons between two groups were conducted using the Student t test, whereas multiple groups were analysed using a 1-way analysis of variance (ANOVA). Only values of $p < 0.05$ were considered significant.

Results

Differential gene expression in perfused rat liver following hypoosmolarity-induced cell swelling
The effect of hypoosmotic exposure on the liver transcriptome was studied in perfused rat liver by microarray (Fig. 1 and Fig. S1). Relative mRNA levels at 120 min (Fig. 1A) and 180 min (Fig. 1B) of hypoosmotic conditions were compared with the respective mRNA level under normoosmotic conditions. After 120 min of hypoosmotic perfusion, an upregulation of 351 genes was observed, while 205 genes were downregulated compared with normoosmotic perfused rat liver (Fig. 1A). After 180 min of hypoosmotic exposure, 534 genes were found to be upregulated, and 609 downregulated (Fig. 1B). Comparing the numbers of overall regulated genes at 120 and 180 min with each other showed an intersection of approximately 24% (Fig. S1A). Between the 351 genes upregulated after 120 min and the 534 genes upregulated after 180 min, there was an overlap of 148 genes (Fig. S1B). Between the 205 downregulated genes after 120 min and the 609 genes downregulated after 180 min, the overlap was 196 genes (Fig. S1C). A hierarchical clustering of significantly
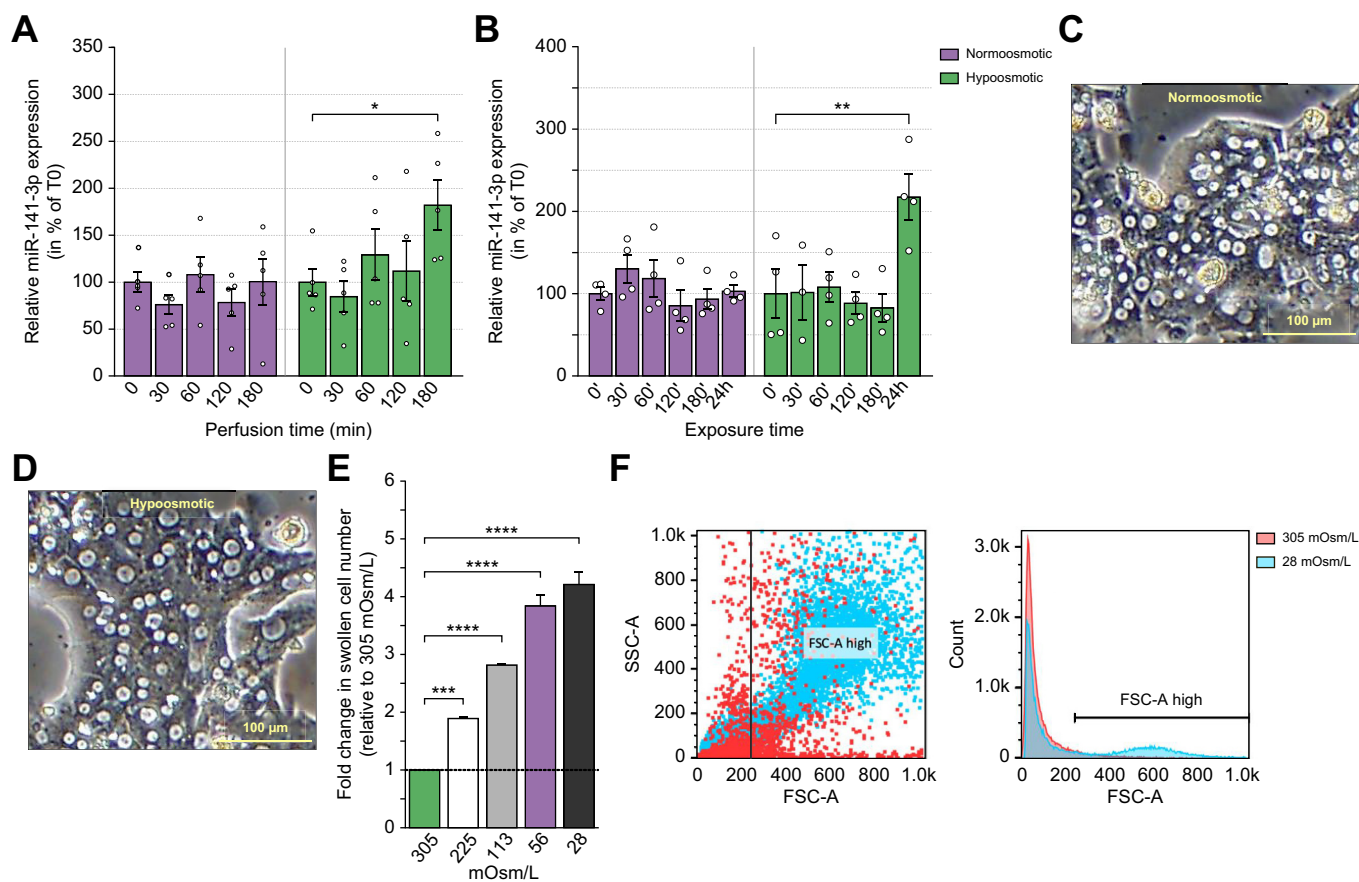
Fig. 3. miQPCR analysis of miR-141-3p in perfused rat livers and isolated rat primary hepatocytes in response to normo- or hypoosmotic exposure. (A) Rat livers were perfused with normo- (305 mOsm/L) or hypoosmotic medium (225 mOsm/L) for up to 180 min. Livers were dissected and the miRNA was analysed by miQPCR (n = 5, ANOVA). (B) Isolated rat primary hepatocytes were exposed to normo- (305 mOsm/L) or hypoosmotic medium (225 mOsm/L) over a time course of 24 h. The miRNA was analysed by miQPCR (n = 4, ANOVA). Microscopic images of rat primary hepatocytes, which were exposed to (C) normo- (305 mOsm/L) or (D) hypoosmotic medium (225 mOsm/L) for 5 min. (E) Freshly isolated rat hepatocytes were resuspended in medium of indicated osmolarity and incubated at 37°C for 5 min directly before flow cytometric analysis of 50,000 cells. Hypoosmolarity caused cell swelling, and this effect was evident at 225 mOsm/L. (F) Representative scatter and histogram plots of primary rat hepatocyte preparations at 305 and 28 mOsm/L, showing the gate used for all cell populations in (E). Data represent mean ± SEM of 3 rat hepatocyte preparations. Significances were calculated using 1-way ANOVA and Dunnett's multiple comparison test with ***p <0.001 and ****p <0.0001. FSC-A, area of forward scatter; SSC-A, area of side scatter.

regulated genes was observed under hypoosmotic conditions in rat liver (Fig. 1C and D).

qPCR validation of hypoosmolarity-regulated mRNAs differentially expressed in microarray analysis

To validate the observed gene expression changes, qPCR analyses were carried out using RNA isolated from rat livers perfused with normo- or hypoosmotic medium for 180 min based on their expression changes in the microarray (Fig. 1B) and on the involvement of known osmosignalling pathways. As shown in Fig. 2A, multiple mRNAs were significantly upregulated under hypoosmotic conditions in rat liver perfusion after 180 min. *Carnitine palmitoyltransferase 2* (*Cpt2*) mRNA was significantly upregulated by 1.87-fold (±0.3), while the *α subunit of the epithelial sodium channel ENaC* (*Scnn1a*) mRNA was upregulated by 11.7-fold (±2.2) under hypoosmotic exposure. Several other mRNAs, including *TIMP metallopeptidase inhibitor 1* (*Timp1*) mRNA, a matrix metalloproteinase inhibitor that inhibits degradation of the extracellular matrix (ECM), *Dual oxidase maturation factor 2* (*Duoxa2*) mRNA, and *N-acetylglutamate synthase* (*Nags*) mRNA, a mitochondrial enzyme that plays a role in the regulation of

ureagenesis, were also found to be significantly upregulated. qPCR was carried out for genes involved in osmosignalling pathways such as the *transcription factor EB* (*Tfeb*). *Tfeb* mRNA was significantly downregulated to 0.33-fold (±0.13) under hypoosmotic conditions compared with normoosmotic control conditions (Fig. 2B). Several other mRNAs were likewise downregulated under hypoosmotic conditions, including those that play important roles in cell cycle progression and microtubule formation, for example mRNAs encoding for *dual serine/threonine and tyrosine protein kinase* (*Dstyk*), a *member of the RAS oncogene family* (*Rab30*), *cell division cycle 25A* (*Cdc25a*), and *nuclear factor of activated T cells 5* (*Nfat5*) (Fig. 2B). Strikingly, these transcripts also harbour and share a common binding motif for miR-141-3p (Fig. S2). Our Affymetrix Gene Expression Array data in concert with qPCR analysis indicate a relevant impact of hypoosmolarity on gene expression in rat livers.

Hypoosmolarity leads to upregulation of miR-141-3p in perfused rat liver and in rat primary hepatocytes

To assess the link between regulated genes and miRNA target prediction, we investigated the regulation of miR-141-3p in
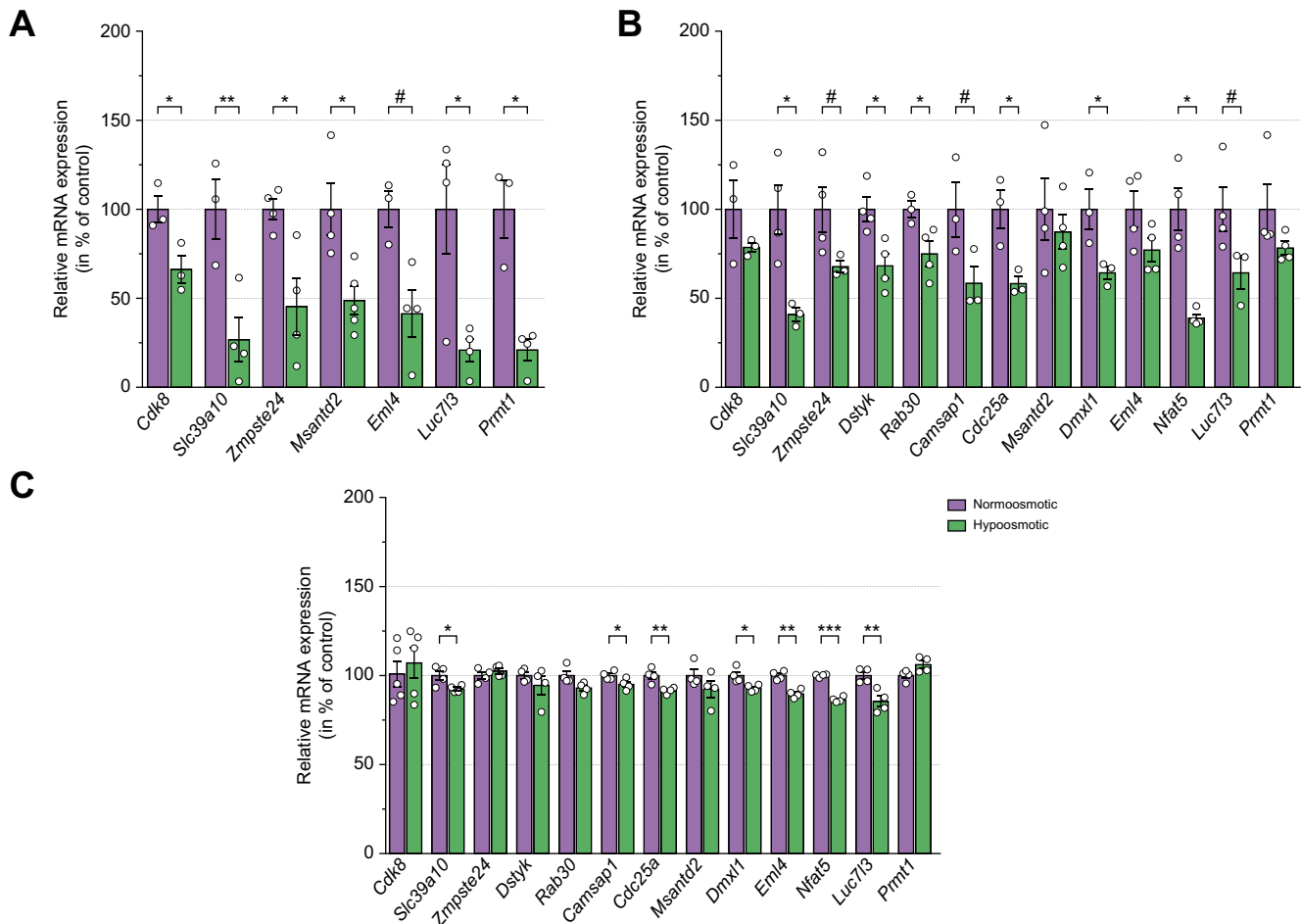
Fig. 4. qPCR analysis of putative target genes of miR-141-3p in perfused rat livers and isolated rat primary hepatocytes in response to normo- or hypoosmotic exposure. (A) Rat livers were perfused with normo- (305 mOsm/L) or hypoosmotic medium (225 mOsm/L) for 180 min. Livers were dissected and mRNA was analysed by qPCR (n = 4). (B) Isolated rat primary hepatocytes were exposed to normo- or hypoosmotic medium for over 24 h. Cells were washed, lysed and the mRNA was analysed by qPCR (n = 4). Relative mRNA levels were normalised to *Rps6* levels. (C) mRNA levels of selected target genes after 120 min of rat liver perfusion were investigated by qPCR (*Cdk8*) and microarray analysis (*Slc39a10, Zmpste24, Dstyk, Rab30, Camsap1, Cdc25a, Msantd2, Dmxl1, Eml4, Nfat5, Luc7l3, Prmt1*). Statistical analysis was carried out using the Student *t* test. Data are shown as mean ± SEM with #*p* <0.1, *p* <0.05, **p* <0.01. *Camsap1*, calmodulin-regulated spectrin-associated protein 1; *Cdc25a*, cell division cycle 25A; *Cdk8*, cyclin dependent kinase 8; *Dmxl1*, Dmx Like 1; *Dstyk*, dual serine/threonine and tyrosine protein kinase; *Eml4*, EMAP like 4; *Luc7l3*, LUC7 like 3 pre-MRNA splicing factor; *Msantd2*, Myb/SANT DNA binding domain containing 2; *Nfat5*, nuclear factor of activated t cells 5; *Prmt1*, protein arginine methyltransferase 1; *Rab30*, member RAS Oncogene Family; *Slc39a10*, solute carrier family 39 member 10; *Zmpste24*, zinc metallopeptidase STE24.

perfused rat liver and rat primary hepatocytes via miQPCR.[22] Based on our target prediction analysis and by applying miR-Walk 3.0 and TargetScan 7.2 on the transcriptome data set, we identified miR-141-3p, which putatively targets the aforementioned *Dstyk*, *Rab30*, *Cdc25a*, and *Nfat5* mRNAs, to be significantly upregulated under hypoosmotic conditions in rat liver perfused for 180 min. Further target predictions showed that miR-141-3p potentially interacted with 249 out of 609 downregulated mRNAs (Fig. S3A). In addition, 170 potential miR-141-3p targets were downregulated after 180 min, but not after 120 min, whereas the overlap between concordantly downregulated miR-141-3p targets after 120 and 180 min was 79 mRNAs (Fig. S1D). Significant upregulation of miR-141-3p was observed after 180 min of hypoosmolarity (1.8-fold; *p* = 0.033) as compared with the preperfusion state (defined as T0), while the expression levels under normoosmotic conditions remained stable in perfused liver (Fig. 3A). We then quantified miR-141-3p expression in rat primary hepatocytes under hypoosmotic conditions and found

that the miR-141-3p was significantly upregulated in rat primary hepatocytes after 24 h of hypoosmotic exposure, whereas it remained stable within 3 h of hypoosmolarity and in the normoosmotic control during the whole experiment (*i.e.* up to 24 h) (Fig. 3B). To investigate whether treatment with hypoosmolarity indeed induces cell swelling (Fig. 3C,D), cell enlargement was assessed by flow cytometry. A decrease in osmolarity from 305 to 225 mOsm/L led to a significant increase in the number of swollen cells (Fig. 3E,F).

Potential target genes of miR-141-3p are downregulated during hypoosmotic exposure

Our bioinformatic analyses using the TargetScan 7.2 database and miRWalk 3.0 revealed additional putative target mRNAs of miR-141-3p such as *cyclin-dependent kinase 8* (*Cdk8*), *zinc metallopeptidase STE24* (*Zmpste24*), *solute carrier family 39 member 10* (*Slc39a10*), and *LUC7 like 3 pre-mRNA splicing factor* (*Luc7l3*). To investigate whether these putative miR-141-3p target genes
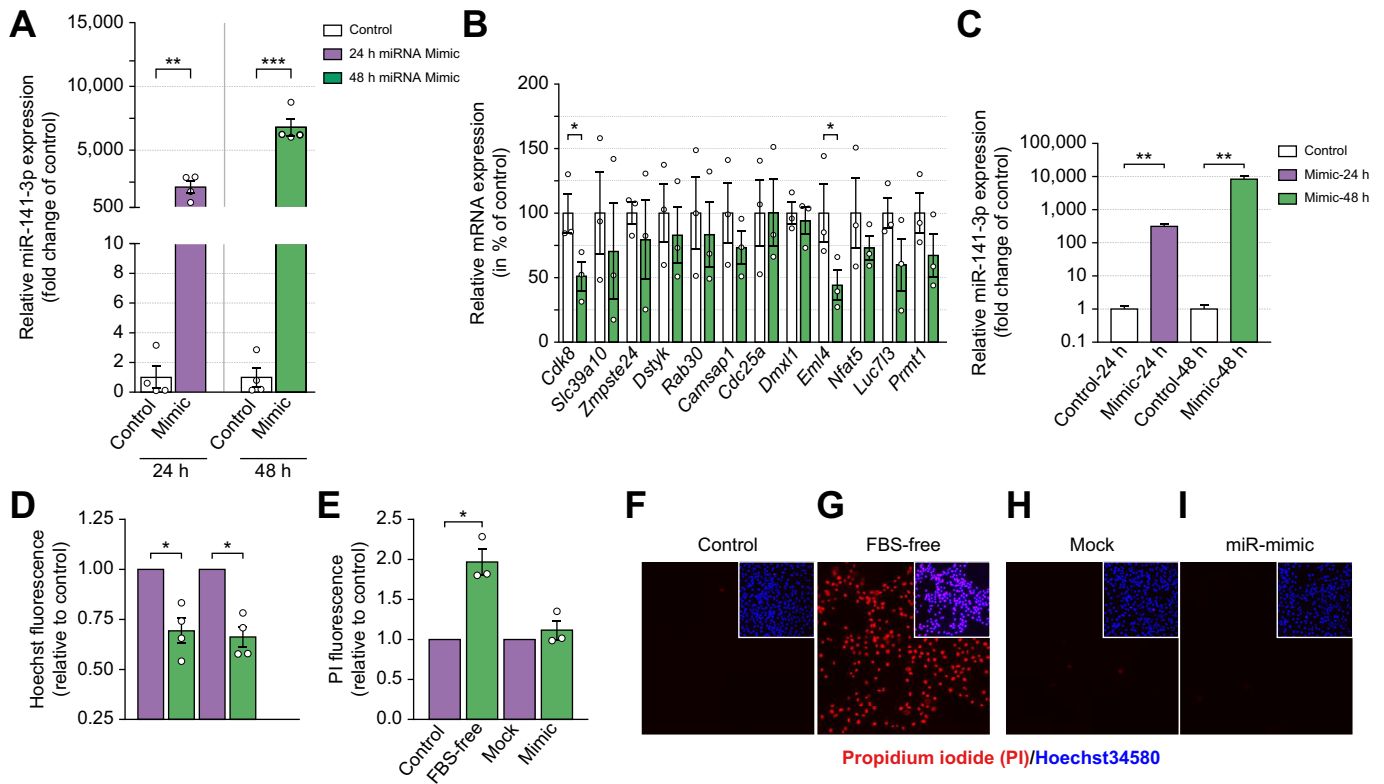
Fig. 5. Analysis of potential target genes 48 h after transfection of miR-141-3p mimic in rat primary hepatocytes and functional analysis. Isolated rat primary hepatocytes were transfected with miR-141-3p mimic or mock (control). After 24 and 48 h, the miRNA (A) and mRNA (B) were analysed by miQPCR and qPCR, respectively. (C) miRNA levels measured by miQPCR in transfected Huh7 cells. miQPCR data were median-normalised, qPCR data were normalised to *Rps6* mRNA levels. (D–I) Effects of miR-141-3p mimic transfection on Huh7 cell proliferation and viability. Proliferation was measured by quantifying the DNA content by fluorimetric detection of Hoechst 34580 fluorescence. Huh7 cell viability was assessed by propidium iodide staining and fluorescence microscopy. Nuclei were counterstained using Hoechst 34580 (F–I). Statistical analysis was carried out using the Student *t* test. (n = 3–4, data are shown as mean ± SEM with *p <0.05, **p <0.01 and ***p <0.001; n.s.: not significant). *Camsap1*, calmodulin-regulated spectrin-associated protein 1; *Cdc25a*, cell division cycle 25A; *Cdk8*, cyclin dependent kinase 8; *Dmxl1*, Dmx Like 1; *Dstyk*, dual serine/threonine and tyrosine protein kinase; *Eml4*, EMAP like 4; *Luc7l3*, LUC7 like 3 pre-mRNA splicing factor; *Nfat5*, nuclear factor of activated t cells 5; *Prmt1*, protein arginine methyltransferase 1; *Rab30*, member RAS Oncogene Family; *Slc39a10*, solute carrier family 39 member 10; *Zmpste24*, zinc metallopeptidase STE24.

are dysregulated in response to hypoosmotic conditions, qPCR analysis was carried out for predicted target genes identified in rat liver tissue exposed to hypoosmolarity (Fig. 4A). In rat primary hepatocytes exposed to hypoosmotic exposure, putative target mRNAs of miR-141-3p were downregulated after 24 h (Fig. 4B). In concert with the data in hypoosmotic perfused rat liver (Fig. 4A), several mRNAs were downregulated in rat primary hepatocytes exposed to hypoosmolarity, that is *Slc39a10*, *Zmpste24*, *Rab30*, *Camsap1* (calmodulin-regulated spectrin-associated protein 1), *Cdc25a*, *Dmxl1* (Dmx Like 1), *Nfat5*, and *Luc7l3* mRNAs (Fig. 4B). Interestingly, GO analysis of down-regulated mRNAs in the transcriptome-wide analysis putatively targeted by miR-141-3p (Fig. S3A) revealed an enrichment of various GO terms associated with the regulation of metabolism, chromatin organisation, positive regulation of cell proliferation, and biosynthetic processes (Fig. S3B).

Transfection of miR-141-3p mimic results in Cdk8, Eml4, and Nfat5 mRNA downregulation in rat primary hepatocytes and inhibits proliferation in Huh7 cells

After validation of miR-141-3p upregulation in rat primary hepatocytes under hypoosmolarity (Fig. 3B), miR-141-3p mimic transfection in rat primary hepatocytes was carried out (Fig. 5A) and the expression of target genes was then measured after 24 h

(Fig. S4) and 48 h (Fig. 5B). As shown in Fig. 5B, the mRNA of the putative miR-141-3p target *Nfat5* decreased after 24 h (p = 0.067, Fig. S4), and the mRNAs of the putative targets *Cdk8* and *Eml4* (EMAP like 4) were significantly reduced 48 h after miR-141-3p mimic transfection in rat primary hepatocytes (Fig. 5B). Trans-fecting Huh7 cells with miR-141-3p mimic inhibited prolifera-tion by about 40% compared with mock-transfected cells (Fig. 5D) but did not affect their viability, as indicated by un-changed propidium iodide (PI) uptake (Fig. 5E–I). Culturing Huh7 cells in FBS-free medium inhibited cell proliferation to a similar extent, as found in miR-141-3p mimic-transfected cells (Fig. 5D), and strongly increased the uptake of PI (Fig. 5E–I). This indicates that growth factor withdrawal impairs the viability of cultured Huh7 cells.

Src-mediated activation of Erk/p38 is required to activate the expression of miR-141-3p, and the upregulation of miR-141-3p by hypoosmolarity is abolished after application of colchicine

Hypoosmotic exposure results in activation of Src-kinase and subsequent activation of Erk/p38 downstream kinases.[31] To investigate the potential role of these osmosensing signalling cascades, we conducted rat liver perfusion with Src (PP-2), Erk (PD098059), and p38 (PD169316) inhibitors. In normoosmotic
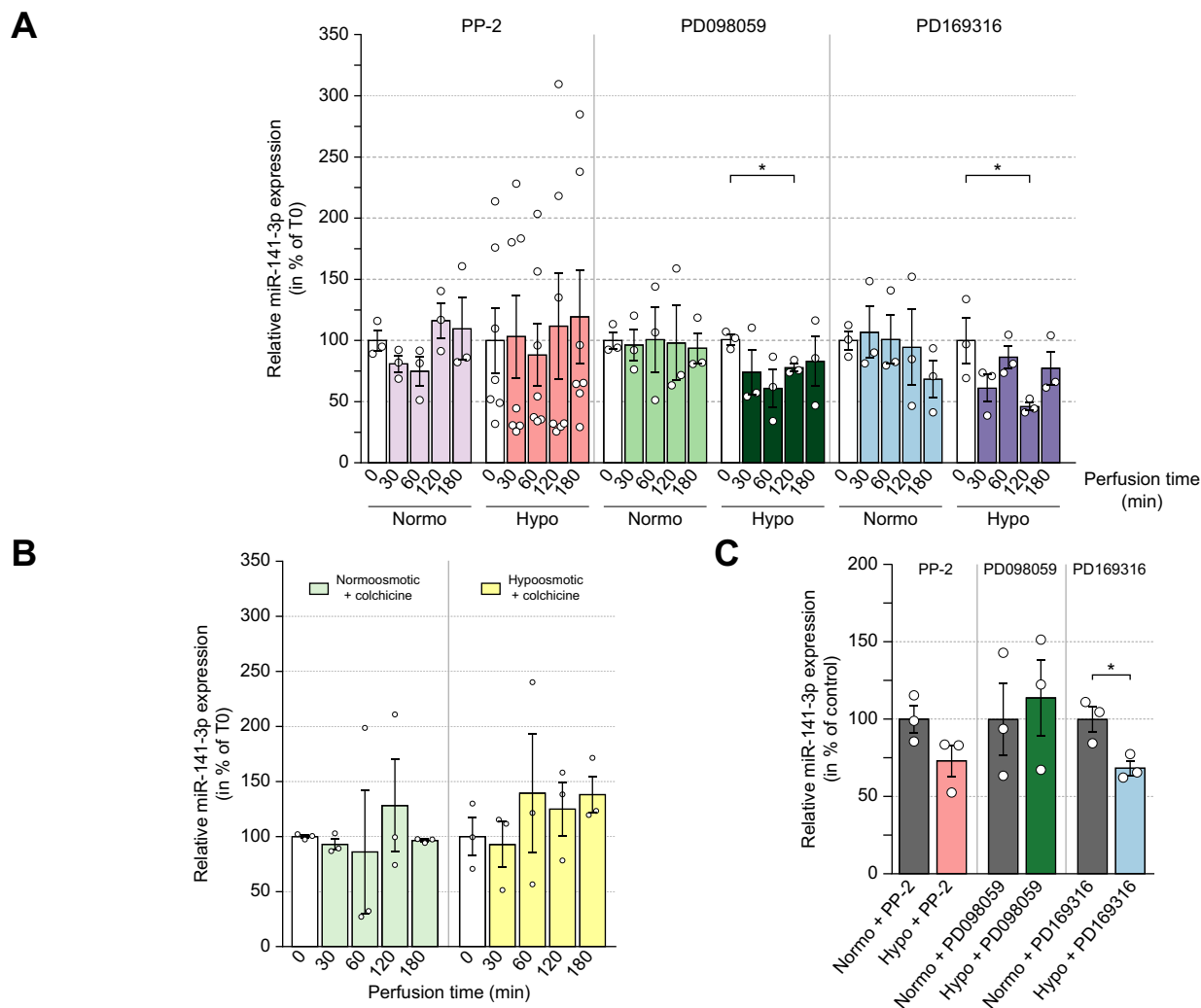
Fig. 6. Analysis of miR-141-3p expression by hypoosmolarity in presence of Src-, Erk-, p38-inhibitors, and colchicine. Rat livers were perfused with normo- (305 mOsm/L) or hypoosmotic (225 mOsm/L) medium for 0–180 min. (A) Inhibitors of Src (PP-2), Erk (PD098059), p38 (PD169316), or colchicine (B) were added to the perfusate as indicated. After perfusion, the miR-141-3p amount was quantified by miQPCR. Data represent the relative expression of miR-141-3p as a percentage to the preperfusion state (T0). (C) Quantification of miR-141-3p at 24 h after treatment of primary hepatocytes with PP-2, PD098059, and PD169316 under normo- und hypoosmotic condition (n = 3). Statistical analysis was carried out using 1-way ANOVA. (n = 3–7, data are shown as mean ± SEM with *p <0.05).

control, adding PP-2 to the perfusate had no significant effect on miR-141-3p levels. The addition of PP-2 to the hypoosmotic buffer prevented miR-141-3p upregulation (Fig. 6A, left). Furthermore, supplementation of PD098059 to the hypoosmotic perfusion buffer resulted in a transient downregulation of miR-141-3p after 60 min of hypoosmotic exposure, while miR-141-3p remained stable under normoosmotic control, containing PD098059 during the entire period (Fig. 6A, middle). These data suggest that miR-141-3p upregulation by hypoosmolarity is initiated downstream of Erk. Further inhibitor experiments with PD169316 were carried out in perfused rat liver and revealed that upregulation of miR-141-3p by hypoosmolarity was abolished by p38-MAPK inhibition (Fig. 6A, right).

To further investigate the involvement of miR-141-3p in the hypoosmolarity-induced effects on liver cells, that is the inhibition of proteolysis,[32] we analysed the effect of colchicine added to normo- and hypoosmotic perfusion buffers. Colchicine is a well-known microtubule inhibitor that exerts effects downstream of p38-MAPK.[33] After the addition of colchicine to the

perfusate, hypoosmolarity-induced miR-141-3p upregulation was prevented, whereas no effect was observed on miR-141-3p in livers perfused with normoosmotic buffers in the presence of colchicine (Fig. 6B).

Inhibition of Src (PP-2), Erk by inhibition of MEK1/2 (PD098059) and p38 (PD169316) inhibited miR-141-3p upregulation by hypoosmolarity in primary hepatocytes after 24 h (Fig. 6C).

Cdk8 3′-UTR is directly regulated by miR-141-3p

To assess the potential interaction between miR-141-3p and *Cdk8,* we conducted bioinformatic analysis using miRWalk 3.0 and TargetScan 7.2. We identified that *Cdk8* mRNA harbors two putative miRNA recognition sites for miR-141-3p within the 3′-UTR (Fig. 7A). To establish whether miR-141-3p directly regulates *Cdk8* mRNA, the full-length 3′-UTR of *Cdk8* was cloned into luciferase reporter plasmids, which were transfected into HEK293 cells. Luciferase reporter assays revealed that cotransfection of HEK293 cells with pMir-Cdk8(+) and miR-141-
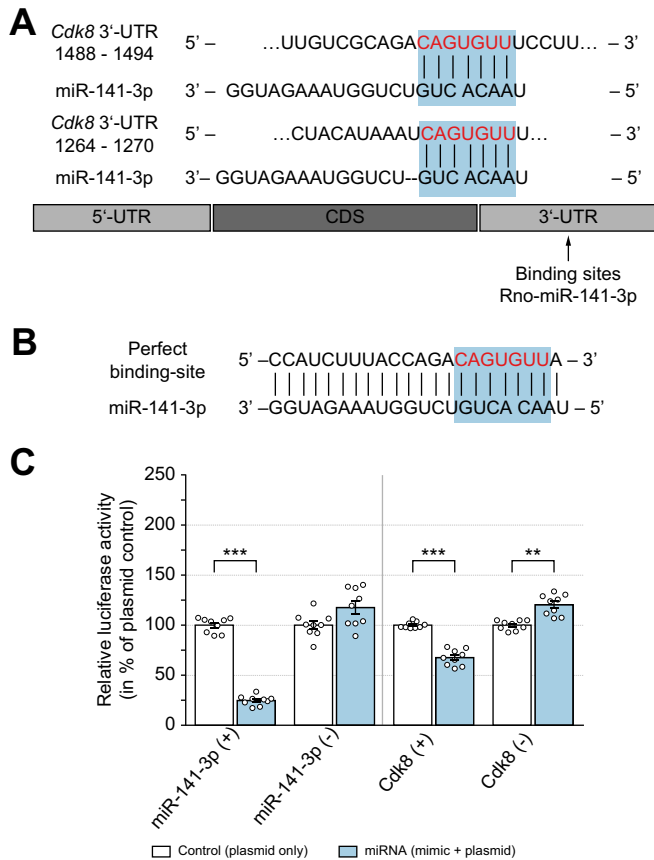
Fig. 7. Validation of rat *Cdk8* 3'-UTR as a direct target site of miR-141-3p by luciferase assay. (A) The predicted duplex formation of *Cdk8* 3'-UTR and miR-141-3p. TargetScan was utilised to predict duplex formation of *Cdk8* 3'-UTR and miR-141-3p. Seed sequence of miR-141-3p is highlighted in the blue box, while the corresponding nucleic acids of *Cdk8* 3'-UTR are displayed in red font. (B) Base pairing of miR-141-3p to its perfectly complementary binding site. (C) HEK293 cells were transfected with recombinant plasmids either in absence (black) or in presence of miR-141-3p mimic (blue). Luciferase activity was measured from cell lysates 24 h post-transfection. Data are presented as mean ± SEM of 3 independent experiments. As control, luciferase activity in absence of miR-141-3p was set to 100%. Student *t* test with significance level **p <0.01; ***p <0.001. *Cdk8*, cyclin dependent kinase 8.

3p mimics caused a notable decrease in luciferase activity to 0.68-fold (±0.03) in comparison with pMir-Cdk8(+) absent miR-141-3p mimics (p <0.05; Fig. 7C). No reduction in luciferase activity was observed when miR-141-3p mimics were co-transfected with the recombinant plasmid pMir-Cdk8(-), which encoded for the 3'-UTR of *Cdk8* mRNA in inverse orientation. Collectively, these data support our conclusion that miR-141-3p directly interacts with *Cdk8* 3'-UTR.

Potential involvement of miR-141-3p and its target gene Cdk8 in liver regeneration

Partial hepatectomy (PHx) is a well-established procedure to induce liver regeneration and hepatocyte proliferation after removing two-thirds of the liver.[20] As miR-141-3p plays a role in cell proliferation,[34] expression levels of miR-141-3p and its putative target *Cdk8* mRNA were analysed in the livers of rats recovering from PHx. The miR-141-3p was significantly upregulated by 2.5-fold (±0.5) 3 days after PHx compared with the uninjured liver (T0) (Fig. 8A), whereas *Cdk8* mRNA was significantly downregulated, evidenced by a 0.5-fold (±0.1) decrease 6 days after PHx (Fig. 8B). These findings suggest that miR-141-3p could play a role in the control of hepatocyte proliferation, which is known to peak in rat liver 24 h after PHx.[35]

Compression, tension, and stretching of liver cells all occur in hypoosmotic-induced cell swelling and during liver regeneration, thus resulting in mechanical stimulation of liver cells. To gain further insights into the potential factors that enable upregulation of miR-141-3p, we investigated rat primary hepatocytes exposed to mechanical stimulation. For this purpose, isolated rat primary hepatocytes were seeded on flexible thin silica membrane chambers coated with ECM proteins. The silicone elastomer allowed the appliance of a tractive force, resulting in a cell stretching of approximately 30%. Mechanical stimulation of primary rat hepatocytes by stretching (Fig. 8E–H) resulted in an upregulation of miR-141-3p by 9.6-fold (±1.4) after 1 h (Fig. 8I), which successively decreased again during culture time. *Cdk8* mRNA levels were downregulated to 0.72-fold (±0.13; p = 0.164) and to 0.75-fold (±0.10; p = 0.127), respectively, 2 and 3 h after mechanical stimulation by stretching (Fig. 8J).

Discussion

Many cellular functions are dependent on cell volume, ionic strength of the cytoplasm, and macromolecular crowding,[36] where macromolecular crowding refers to the behaviour of proteins within the cell with respect to the water and salt content of the cytoplasm.[37] In the present study, we identified differentially expressed genes in rat livers perfused with hypoosmotic medium compared with normoosmotic medium. Important genes involved in cell proliferation were validated by qPCR and further investigated based on target prediction algorithms. Genes that were shown to be dysregulated under hyperosmotic stress, for example *Nfat5*,[38] showed an opposite regulation under hypoosmotic conditions. Downregulated mRNAs were further investigated for potential binding sites of miRNAs to further investigate their role in hypoosmotic-related gene expression.

Here, we identified miR-141-3p as the potential mediator of hypoosmotic-induced gene expression changes. The expression of miR-141-3p was upregulated in perfused rat livers and rat primary hepatocytes in response to hypoosmolarity. Interestingly, hypoosmotic-induced miR-141-3p upregulation was observed only after 24 h in cell culture experiments, whereas it occurred within 3 h in perfused rat livers. The discrepancies between the observed effects could be explained by the biological cell matrix, which is missing in the cell culture system but present in the perfusion experiment. In addition, ~3.7% (249/6,793) of the predicted miR-141-3p target genes were downregulated in rat livers perfused with hypoosmotic medium. The time course of target mRNA degradation by miR-141-3p may be mRNA species-specific. However, the isolated liver perfusion method is technically limited to a perfusion time of 180 min.[39]

The hypoosmotic-induced upregulation of miR-141-3p was prevented in the presence of Src inhibitor. Inhibition of Erk and p38 resulted in a significant downregulation of miR-141-3p after 120 min, indicating that miR-141-3p is regulated downstream to Erk and p38 MAPK. As Src, Erk and p38 are well-known downstream effectors of hypoosmotic-induced signalling pathways, these findings further suggest that miR-141-3p may be directly involved in cellular response to hypoosmotic conditions. Here, it
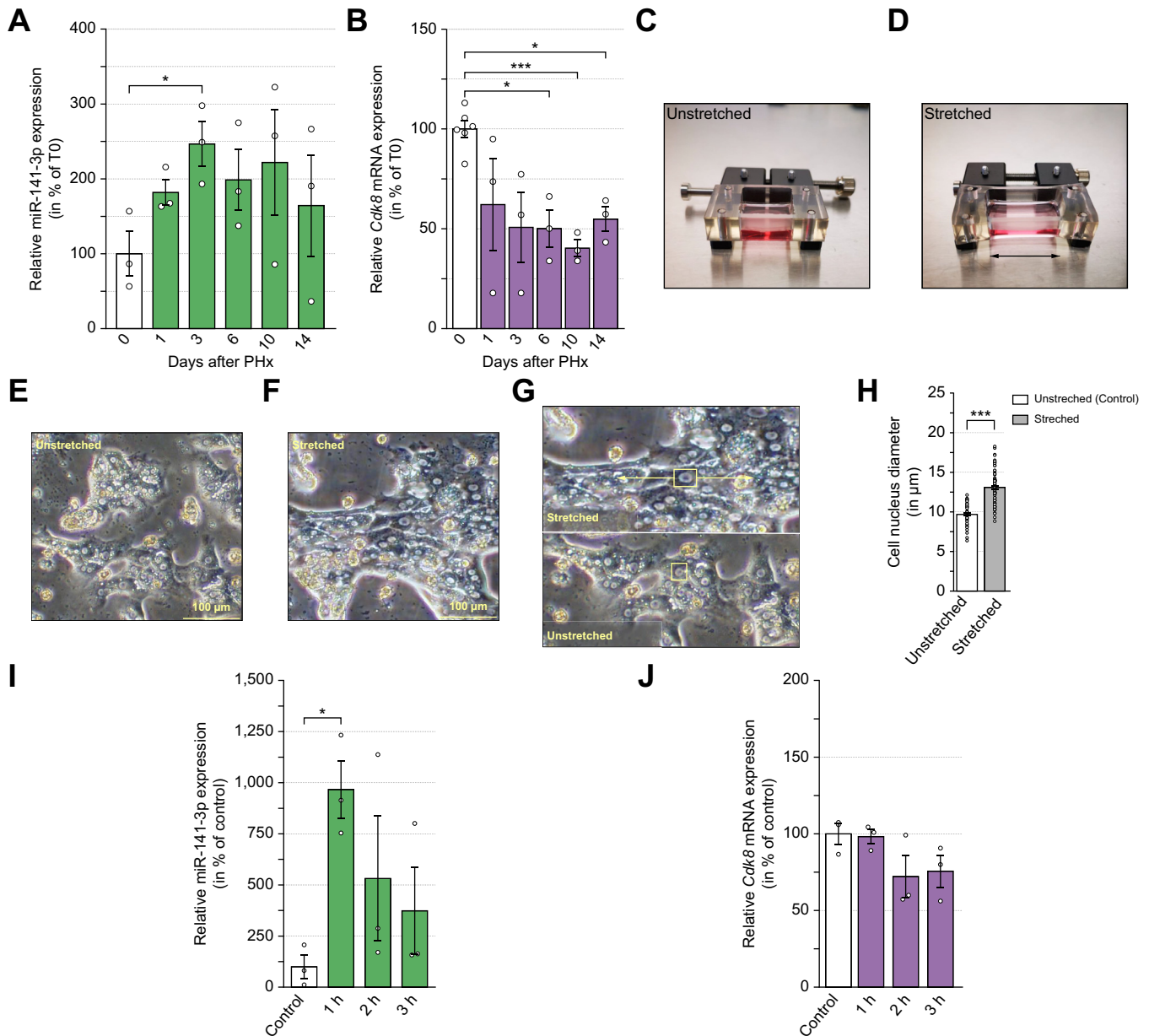
Fig. 8. Effects of PHx and mechanical stimulation on the expression of miR-141-3p in rat. Rats at the age of 8–10 weeks were subjected to PHx. Rats were sacrificed during liver regeneration at indicated times (0–14 days). Hepatic RNA was isolated and levels of miR-141-3p and *Cdk8* mRNA were analysed by miQPCR and qPCR, respectively. (A) Levels of miR-141-3p in the livers of rats that underwent PHx. Data were normalised by median normalisation (n = 3–6, one-way ANOVA). (B) Relative *Cdk8* mRNA levels in the livers of rats subjected to PHx. qPCR data were normalised to *Rps6* mRNA levels (n = 3–6, one-way ANOVA). Images of silicone chambers containing hepatocytes that (C) remain unstretched or were (D) stretched for 1 h. Microscopic images of rat hepatocytes in silicone chambers without (E) or with (F) stretching. To determine the scope of unidirectional cell stretching, the nuclei diameters of hepatocytes were measured at the furthest points, using the software cellSens Dimension. (G) Cell nuclei of unstretched and stretched hepatocytes are depicted in yellow rectangles. (H) Comparison of cell nuclei diameter between unstretched and stretched rat hepatocytes (n = 81, Student *t* test). (I) miR-141-3p amounts in rat hepatocytes subjected to stretching over a time course of 3 h. (J) Levels of *Cdk8* mRNA in rat hepatocytes after stretching for 3 h. (n = 3, 1-way ANOVA). Data are shown as mean ± SEM with *p <0.05, **p <0.01, and ***p <0.001. *Cdk8*, cyclin dependent kinase 8; PHx, partial hepatectomy.

is also reported that the addition of colchicine to the perfusate prevented an upregulation of miR-141-3p under hypoosmotic conditions. Colchicine is known to induce depolymerisation of the microtubule network,[40,41] suggesting a possible involvement of miR-141-3p in microtubule formation and the induced inhibition of proteolysis found during liver cell swelling.[42] Altogether, these data point toward an involvement of miR-141-3p in

the osmosignalling pathways triggered by hypoosmolarity. High variability of miR-141-3p expression in the perfusion experiment with PP-2 could be explained by a lower bioavailability of PP-2. Of note, inhibition of Src (PP-2), Erk (PD098059), and p38 (PD169316) also prevented miR-141-3p upregulation *in vitro*.

To validate miRNA target gene candidates, we identified *Cdk8* mRNA as a direct target of miR-141-3p. *Cdk8* mRNA was

downregulated during hypoosmolarity, while miR-141-3p was upregulated. As a component of the Mediator complex, Cdk8 is involved in the transcription regulation of nearly all RNA polymerase II-dependent genes.[43] Originally, *Cdk8* was identified as an oncogene in colon cancer,[44] whereas C*dk8* protein activity was reported to be involved in the regulation of transcription in several pro-carcinogenic signalling pathways, such as the Wnt/β-catenin[44] and TGFβ/BMP pathways.[45] We validated *Cdk8* mRNA as a direct target of miR-141-3p by identifying 2 possible binding sites located in the 3′-UTR and by functionally validating these binding sites by luciferase reporter assays. In addition, miR-141-3p upregulation and *Cdk8* mRNA reduction were simultaneously found 3 days after PHx, indicating a possible involvement of miR-141-3p and *Cdk8* in hepatocyte proliferation. The timing of maximal hepatocyte proliferation on Day 1 of regeneration after PHx, and the subsequent increase of miR-141-3p may indicate this miRNA has a regulatory function that contributes to terminating liver regeneration. In addition, the mechanical stretching of rat primary hepatocytes triggered by PHx, because the blood volume from the portal vein passes through only one-third of the remaining liver tissue,[46] also resulted in a substantial upregulation of miR-141-3p, as demonstrated in the present study. Additionally, mechanical stretching of rat primary hepatocytes also resulted in the upregulation of miR-141-3p. Mechanical cues initiate cell proliferation on the one hand, but must be tightly controlled on the other hand, to prevent excessive hepatocyte growth during liver repair. These findings may point toward a counter-regulatory antiproliferative response, because miR-141-3p inhibits cell proliferation but does not decrease the viability of Huh7 cells as demonstrated herein. However, in other tumour cells this mechanism is probably altered, because recent studies have shown that miR-141-3p enhances proliferation in ovarian cancer,[47] and silencing of miR-141-3p inhibits proliferation of JEG-3 choriocarcinoma cells.[48] miR-141-3p was also shown to promote prostate cancer cell proliferation and inhibit cell apoptosis.[49]

In line with this, *Cdk8* mRNA expression tended to decrease in hepatocytes after mechanical stimulation, but not significantly. Furthermore, it was demonstrated that hypoosmolarity induces hepatocyte swelling after 5 min incubation. However, not all hepatocytes showed a significant swelling response within that time. Although the viability of cells after preparation was good (>90% in all 3 preparations as determined by Trypan Blue exclusion; not shown), damaged or dying cells may also be included in flow cytometry analyses. Here, we refrained from using viability dyes such as DAPI and propidium iodide because hypoosmolarity can be used to mediate cellular uptake of otherwise membrane-impermeable compounds into viable cells.[50] Preparation by collagenase perfusion results in a mixture of liver cell types (parenchymal, endothelial, biliary, immune cells) with hepatocytes being the vast majority. To cope with complexity, a gate was set to identify swollen cells based on the osmolarity-induced differences in the FSC-A histograms.

When gene expression in isolated primary hepatocytes exposed to hypoosmotic medium were compared with hepatocytes transfected with miR-141-3p mimic, there was little overlap. This could be because hypoosmolarity triggers further gene expression changes, which may interfere with miR-141-3p-induced gene expression changes. Integrins, which belong to the family of transmembrane glycoproteins, are osmo- and mechanical sensors in the liver. Following activation, they mediate the Src- and MAP-kinase activation induced by hypoosmotic swelling,[45] which ultimately leads to proliferation.[17] Here, we showed that miR-141-3p was upregulated following cell stretching and under hypoosmotic conditions, and that the inhibition of either Src-, p38-MAPK, or Erk largely prevented the increase in miR-141-3p levels. The aforementioned MAPK-mediated signals that trigger cell proliferation may increase miR-141-3p to provide a negative feedback loop. Whereas the data presented in this study point toward a central role of miR-141-3p in osmo- and mechanical sensing of hepatocytes, conditional gene knockout experiments are still needed to elucidate the involvement and functional relevance of miR-141-3p and *Cdk8* as regulatory elements of the regenerative liver.

Abbreviations

Camsap1, calmodulin-regulated spectrin-associated protein 1; *Cdc25a*, cell division cycle 25A; *Cdk8*, cyclin dependent kinase 8; *Cpt2*, carnitine palmitoyl transferase 2; *Dmxl1*, Dmx Like 1; *Dstyk*, dual serine/threonine and tyrosine protein kinase; *Duoxa2*, dual oxidase maturation factor 2; ECM, extracellular matrix; *Eml4*, EMAP like 4; GO, gene ontology; *Gucy2c*, guanylate cyclase 2C; *Luc7l3*, LUC7 like 3 pre-mRNA splicing factor; *miRNA*, microRNA; *Msantd2*, Myb/SANT DNA binding domain containing 2; *Nags*, N-acetyl glutamate synthase; *Nfat5*, nuclear factor of activated t cells 5; PHx, partial hepatectomy; PI, propidium iodide; *Prmt1*, protein arginine methyltransferase 1; qPCR, quantitative PCR; *Rab30*, member RAS Oncogene Family; *Rps6*, ribosomal Protein S6; RT, room temperature; *Scnn1a*, sodium channel epithelial 1 subunit alpha; *Slc39a10*, solute carrier family 39 member 10; *Tfeb*, transcription factor EB; *Timp1*, tissue inhibitor of metalloproteinase 1; *Zmpste24*, zinc metallopeptidase STE24.

Conflicts of interest

The authors have declared no conflicts of interest.

Please refer to the accompanying ICMJE disclosure forms for further details.

Authors' contributions

Designed and planned the research: DS. Analysed the Affymetrix data: NB, MC, DS. Isolated RNA, performed miQPCR and qPCR, performed bioinformatic analyses and analysed the data: DS, NB. Contributed to research: MP, MC, CK, BG, JS, TL, SvD, DH. Carried out partial hepatectomy: CK. Conducted and analysed proliferation and viability assays in Huh7 cells: BG. Conducted FACS analysis: JS. Wrote the manuscript: all authors.

Data availability statement

The data that support the findings of this study are available on request from the corresponding author and the Department of Gastroenterology, Hepatology and Infectious Diseases, University Hospital Düsseldorf (Wissenschaft.Gastro@med.uni-duesseldorf.de). The results of the Affymetrix microarray data are deposited in the GEO (Gene Expression Omnibus) NCBI database and are accessible under the number GSE183462.

References

Author names in bold designate shared co-first authorship

[1] Häussinger D. The role of cellular hydration in the regulation of cell function. Biochem J 1996;313:697–710.

[2] Lang F, Busch GL, Ritter M, Völkl H, Waldegger S, Gulbins E, et al. Functional significance of cell volume regulatory mechanisms. Physiol Rev 1998;78:247–306.

[3] Schliess F, Häussinger D. Cell volume and insulin signaling. Int Rev Cytol 2003;225:187–228.

[4] McManus ML, Churchwell KB, Strange K. Regulation of cell volume in health and disease. N Engl J Med 1995;333:1260–1266.

[5] Häussinger D, Lang F. Cell volume and hormone action. Trends Pharmacol Sci 1992;13:371–373.

[6] **Santosa D**, **Castoldi M**, Paluschinski M, Sommerfeld A, Häussinger D. Hyperosmotic stress activates the expression of members of the miR-15/107 family and induces downregulation of anti-apoptotic genes in rat liver. Sci Rep 2015;5:1–19.

[7] Castoldi M, Spasic MV, Altamura S, Elmén J, Lindow M, Kiss J, et al. The liver-specific microRNA miR-122 controls systemic iron homeostasis in mice. J Clin Invest 2011;121:1386–1396.

[8] Lee S-O, Masyuk T, Splinter P, Banales JM, Masyuk A, Stroope A, et al. MicroRNA15a modulates expression of the cell-cycle regulator Cdc25A and affects hepatic cystogenesis in a rat model of polycystic kidney disease. J Clin Invest 2008;118:3714–3724.

[9] Humphreys KJ, McKinnon RA, Michael MZ. miR-18a inhibits CDC42 and plays a tumour suppressor role in colorectal cancer cells. PLoS One 2014;9:e112288.

[10] Leung AKL, Sharp PA. MicroRNA functions in stress responses. Mol Cell 2010;40:205–215.

[11] Esquela-Kerscher A, Slack FJ. Oncomirs – microRNAs with a role in cancer. Nat Rev Cancer 2006;6:259–269.

[12] Nigi L, Grieco GE, Ventriglia G, Brusco N, Mancarella F, Formichi C, et al. MicroRNAs as regulators of insulin signaling: research updates and potential therapeutic perspectives in type 2 diabetes. Int J Mol Sci 2018;19:3705.

[13] O'Hara SP, Gradilone SA, Masyuk TV, Tabibian JH, LaRusso NF. MicroRNAs in cholangiopathies. Curr Pathobiol Rep 2014;2:133–142.

[14] **Flynt AS**, **Thatcher EJ**, Burkewitz K, Li N, Liu Y, Patton JG. miR-8 microRNAs regulate the response to osmotic stress in zebrafish embryos. J Cell Biol 2009;185:115–127.

[15] Huebert RC, Jagavelu K, Hendrickson HI, Vasdev MM, Arab JP, Splinter PL, et al. Aquaporin-1 promotes angiogenesis, fibrosis, and portal hypertension through mechanisms dependent on osmotically sensitive microRNAs. Am J Pathol 2011;179:1851–1860.

[16] Häussinger D, Reinehr R. Osmotic regulation of bile acid transport, apoptosis and proliferation in rat liver. Cell Physiol Biochem 2011;28:1089–1098.

[17] Reinehr R, Sommerfeld A, Häussinger D. Insulin induces swelling-dependent activation of the epidermal growth factor receptor in rat liver. J Biol Chem 2010;285:25904–25912.

[18] Meijer AJ, Gimpel JA, Deleeuw GA, Tager JM, Williamson JR. Role of anion translocation across the mitochondrial membrane in the regulation of urea synthesis from ammonia by isolated rat hepatocytes. J Biol Chem 1975;250:7728–7738.

[19] **Eden E**, **Navon R**, Steinfeld I, Lipson D, Yakhini Z. GOrilla: a tool for discovery and visualization of enriched GO terms in ranked gene lists. BMC Bioinformatics 2009;10:48.

[20] Higgins GM, Anderson RM. Experimental pathology of liver: restoration of liver of white rat following partial surgical removal. AMA Arch Pathol 1931; https://www.scienceopen.com/document?vid=a5b47d2b-1859-4562-9dd8-f284dccabceb. [Accessed 11 August 2021].

[21] Sies H. The use of perfusion of liver and other organs for the study of microsomal electron-transport and cytochrome P-450 systems. Methods Enzymol 1978;52:48–59.

[22] Benes V, Collier P, Kordes C, Stolte J, Rausch T, Muckentaler MU, et al. Identification of cytokine-induced modulation of microRNA expression and secretion as measured by a novel microRNA specific qPCR assay. Sci Rep 2015;5:11590.

[23] Hellemans J, Mortier G, De Paepe A, Speleman F, Vandesompele J. qBase relative quantification framework and software for management and automated analysis of real-time quantitative PCR data. Genome Biol 2007;8:R19.

[24] Kozomara A, Birgaoanu M, Griffiths-Jones S. miRBase: from microRNA sequences to function. Nucleic Acids Res 2019;47:D155–D162.

[25] Zerbino DR, Achuthan P, Akanni W, Amode MR, Barrell D, Bhai J, et al. Ensembl 2018. Nucleic Acids Res 2018;46:D754–D761.

[26] Griffiths-Jones S, Saini HK, van Dongen S, Enright AJ. miRBase: tools for microRNA genomics. Nucleic Acids Res 2008;36:D154–D158.

[27] Korpelainen E, Tuimala J, Somervuo P, Huss M, Wong G. Dual luciferase gene reporter assays to study miRNA function. RNA-Seq Data Anal A Pract Approach 2015;1296:187–198.

[28] Schindelin J, Arganda-Carreras I, Frise E, Kaynig V, Longair M, Pietzsch T, et al. Fiji: an open-source platform for biological-image analysis. Nat Methods 2012;9:676–682.

[29] Görg B, Karababa A, Schütz E, Paluschinski M, Schrimpf A, Shafigullina A, et al. O-GlcNAcylation-dependent upregulation of HO1 triggers ammonia-induced oxidative stress and senescence in hepatic encephalopathy. J Hepatol 2019;71:930–941.

[30] Kiehl TR, Shen D, Khattak SF, Jian Li Z, Sharfstein ST. Observations of cell size dynamics under osmotic stress. Cytometry A 2011;79:560–569.

[31] Schliess F, Kurz AK, vom Dahl S, Häussinger D. Mitogen-activated protein kinases mediate the stimulation of bile acid secretion by tauroursodeoxycholate in rat liver. Gastroenterology 1997;113:1306–1314.

[32] Vom Dahl S, Schliess F, Reissmann R, Görg B, Weiergräber O, Kocalkova M, et al. Involvement of integrins in osmosensing and signaling toward autophagic proteolysis in rat liver. J Biol Chem 2003;278:27088–27095.

[33] vom Dahl S, Dombrowski F, Schmitt M, Schliess F, Pfeifer U, Häussinger D. Cell hydration controls autophagosome formation in rat liver in a microtubule-dependent way downstream from p38MAPK activation. Biochem J 2001;354:31.

[34] **Gao Y**, **Feng B**, Han S, Zhang K, Chen J, Li C, et al. The roles of MicroRNA-141 in human cancers: from diagnosis to treatment. Cell Physiol Biochem 2016;38:427–448.

[35] Taub R. Liver regeneration: from myth to mechanism. Nat Rev Mol Cell Biol 2004;5:836–847.

[36] Parker JC, Colclasure GC. Macromolecular crowding and volume perception in dog red cells. Mol Cell Biochem 1992;114:9–11.

[37] Minton AP, Colclasure GC, Parker JC. Model for the role of macromolecular crowding in regulation of cellular volume. Proc Natl Acad Sci U S A 1992;89:10504–10506.

[38] Lee JH, Kim M, Im YS, Choi W, Byeon SH, Lee HK. NFAT5 induction and its role in hyperosmolar stressed human limbal epithelial cells. Investig Opthalmol Vis Sci 2008;49:1827.

[39] Gores GJ, Kost LJ, LaRusso NF. The isolated perfused rat liver: conceptual and practical considerations. Hepatology 1986;6:511–517.

[40] Brinkley BR, Fistel SH, Marcum JM, Pardue RL. Microtubules in cultured cells; indirect immunofluorescent staining with tubulin antibody. Int Rev Cytol 1980;63:59–95.

[41] Osborn M, Weber K. Cytoplasmic microtubules in tissue culture cells appear to grow from an organizing structure towards the plasma membrane. Proc Natl Acad Sci U S A 1976;73:867–871.

[42] Häussinger D, Stoll B, vom Dahl S, Theodoropoulos PA, Markogiannakis E, Gravanis A, et al. Effect of hepatocyte swelling on microtubule stability and tubulin mRNA levels. Biochem Cell Biol 1994;72:12–19.

[43] Galbraith MD, Donner AJ, Espinosa JM. CDK8: a positive regulator of transcription. Transcription 2010;1:4–12.

[44] Firestein R, Bass AJ, Kim SY, Dunn IF, Silver SJ, Guney I, et al. CDK8 is a colorectal cancer oncogene that regulates β-catenin activity. Nature 2008;455:547–551.

[45] Song W, Wu S, Wu Q, Zhou L, Yu L, Zhu B, et al. The microRNA-141-3p/ CDK8 pathway regulates the chemosensitivity of breast cancer cells to trastuzumab. J Cell Biochem 2019;120:14095–14106.

[46] **Lorenz L**, **Axnick J**, Buschmann T, Henning C, Urner S, Fang S, et al. Mechanosensing by β1 integrin induces angiocrine signals for liver growth and survival. Nature 2018;562:128–132.

[47] Masoumi-Dehghi S, Babashah S, Sadeghizadeh M. microRNA-141-3p-containing small extracellular vesicles derived from epithelial ovarian cancer cells promote endothelial cell angiogenesis through activating the JAK/STAT3 and NF-κB signaling pathways. J Cell Commun Signal 2020;14:233–244.

[48] Morales-Prieto DM, Schleussner E, Markert UR. Reduction in miR-141 is induced by leukemia inhibitory factor and inhibits proliferation in choriocarcinoma cell line JEG-3. Am J Reprod Immunol 2011;66(Suppl. 1):57–62.

[49] Li J, Li J, Wang H, Li X, Wen B, Wang Y. MiR-141-3p promotes prostate cancer cell proliferation through inhibiting kruppel-like factor-9 expression. Biochem Biophys Res Commun 2017;482:1381–1386.

[50] Di Gregorio E, Ferrauto G, Gianolio E, Aime S. Gd loading by hypotonic swelling: an efficient and safe route for cellular labeling. Contrast Media Mol Imag 2013;8:475–486.